

**On the use of crystalline admixtures as promoters of self-healing in cement based construction materials.**

**Liberato Ferrara, Visar Krelani and Fabio Moretti**

**Department of Civil and Environmental Engineering, Politecnico di Milano**

**ABSTRACT**

The project detailed in this paper aims at a thorough characterization of the effects of crystalline admixtures, currently employed as porosity reducing admixtures, on the self-healing capacity of the cementitious composites, i.e. their capacity to completely or partially re-seal cracks and, in case, also exhibit recovery of mechanical properties. The problem has been investigated with reference to both a Normal Strength Concrete (NSC) and a High Performance Fiber Reinforced Cementitious Composite (HPFRCC). In the latter case, the influence of flow-induced fiber alignment has also been considered in the experimental investigation. With reference to either 3-point (for NSC) or 4-point (for HPFRCC) bending tests performed up to controlled crack opening and up to failure, respectively before and after exposure/conditioning recovery of stiffness and stress bearing capacity has been evaluated to assess the self-healing capacity. In a durability-based design framework, self-healing indices to quantify the recovery of mechanical properties will also be defined.

In Normal Strength Concrete, crystalline admixtures are able to promote up to 60% of crack sealing even under exposure to open air. In the case of HPFRCCs, which would already feature autogenous healing capacity because of their peculiar mix compositions, the synergy between the dispersed fiber reinforcement and the action of the crystalline admixture has resulted in a likely “chemical pre-stressing” of the same reinforcement, from which the recovery of mechanical performance of the material has greatly benefited, up to levels even higher than the performance of the virgin un-cracked material.

## 1. Introduction

In our rapidly evolving society sustainability has to become the “ethos” that defines “how we should act, individually and together, to protect and propagate our environment, harness our knowledge, share insights and technologies to build tomorrow while reducing the burden” on today [1].

The field of civil engineering is nowadays characterized by a multifold panorama. On the one hand and mostly even if not exclusively in developing countries, there is a continuously increasing demand for building structures and infrastructure facilities featuring higher and higher levels of performances and not seldom under more and more structurally demanding and environmentally severe service conditions. On the other hand, mostly in developed countries, a larger and larger share of the buildings and infrastructures asset is rapidly approaching its end of service life and is dramatically experiencing a faster and faster deterioration. This requires coordinated policies to be defined and adopted for retrofitting/upgrading interventions (not seldom also because of a modified/increase performance and capacity demand), in which the costs for non-operating periods and related inconveniences should be adequately considered.

*fib* Model Code 2010 has explicitly and firmly recognized sustainability as the “fourth pillar” which has to inform, together with the “classical” requisites of safety, serviceability and durability, the concept, design, construction, maintenance/use and, in case, deconstruction and reuse of any civil and building engineering application.

The porous structure of concrete is one of the main causes of its proneness to degradation. Even if it is generally accepted that a well-proportioned and properly cured concrete, produced using a low water to cement (w/c) ratio, can result in a finished product with good durability, no concrete material and structure can be made absolutely waterproof or “bottle tight”. In fact, because of the porous structure of concrete, water can penetrate through pores and micro-cracks, due to either capillary absorption or (and) hydrostatic pressure. In the first case, the movement of water through the small concrete pores occurs in the absence of any externally applied hydraulic head, as the result

of surface interaction between the water and the pore walls. In the second case, i.e. in the presence of a pressure gradient, the mechanism governing water ingress into concrete and water movement through it is referred to as permeability. It has to be remarked that many concrete professionals use the term permeability to mean the resistance of concrete to water ingress and/or passage under actual service conditions, which include cracked state, as due, e.g., to restrained drying shrinkage and thermal deformations as well as service loads etc.

In the afore pictured framework, together with the already well “acquired” ability to design and cast a concrete as compact and impervious as possible, the engineering community would keenly look for any effective, easily implementable, durable and “repeatable” technology which would make such a concrete also able to activate, upon cracking and damage, self-repairing mechanisms. These mechanisms should also be able to restore, in case, to their pristine level the set of engineering performances, which are relevant to the intended applications [2]. As pointed out by Lauer and Slate already in 1956 [3] “if the mechanism of the action is understood, and means can be found for accelerating it, a great stride will have been made in effectively retarding” the rate of degradation of concrete and corrosion of embedded steel reinforcement, which are among the major problems of the concrete durability [4].

Self-healing materials are inborn into the human body, as witnessed by, e.g., mechanisms of blood clotting, repairing of fractured bones and even by the continuous regeneration of the skeleton cells, which ends up, in average, with a complete renovation of the skeleton as a whole over ten years.

Autogenous healing of concrete was reportedly discovered as early as in 1836 by the French Academy of Science, and attributed to the transformation of calcium hydroxide ( $\text{Ca}(\text{OH})_2$ ) into calcium carbonate ( $\text{CaCO}_3$ ) as a consequence of exposure to the carbon dioxide ( $\text{CO}_2$ ) in the atmosphere. Later, it was also observed by Abrams [5], who attributed it to the “hydraulicity” of residual un-hydrated cement, as well as by Loving [6], who, on inspection of concrete pipe culverts, found many healed cracks filled with calcium carbonate.

As a matter of fact, besides the availability of  $\text{CO}_2$  in the exposure environment, the age of concrete

at the time of cracking also governs the mechanism with the highest autogenous healing capacity. Due to its relatively high content of un-hydrated cement particles, ongoing/delayed hydration is the main healing mechanism in young concrete [7-9], whereas at a later age, calcium carbonate precipitation becomes the major one.

The action of autogenous healing may have “practical value in several applications (...) namely: (...) repair of precast units cracked during early handling; sealing against corrosion and re-knitting of cracks developed in concrete piles during their handling and driving; sealing of cracks in concrete water tanks; and the regain, after loss, of strength of “green” concrete disturbed by vibrations” [10]. Further evidence of the effects of crack healing on the recovery of mechanical properties was reported by Whitehurst [11]. He observed an increase in the dynamic modulus of field structures during a wet spring, following a winter of freezing and thawing. Anyway, whereas significant reduction in water permeability was observed because of crack healing [12-14], reported recovery of mechanical properties [3, 14, 15] was not so spectacular. With reference to the maximum crack width that can be healed without any external intervention, a wide range of openings has been reported by different authors (i.e. from as low as 5 to as high as 300 microns) [16-18].

Consensus among the international community has been achieved about the engineering significance of the problem, which has resulted in state-of-the-art reports to be compiled as well as into a clear terminology definition. The RILEM TC-221-SHC “Self-healing phenomena in cement based materials” [1], distinguishes:

- based on the result of the action, between self-closing and self-healing, whether only closure of the cracks or also restoring of the mechanical properties is observed;
- based on the process of the action, between “autogenic/autogenous” (or natural) and “autonomic” (or engineered) self-closing/healing, whether the crack closure or restoration of material properties is due to either the concrete material itself or some engineered addition.

In the very last decade a huge amount of research work has been dedicated to “engineered” self-

healing, along different directions of investigation: self-healing engineered with fibre reinforcement [20-28], mineral-producing bacteria [29], super absorbent polymers [30], healing agents contained in shell and tubular capsules [31, 32] and other proprietary chemical admixtures [33]. In the latter case, the self-healing action is mainly due to the filling of the crack width, swelling and expansion effects and to improved hydration and re-crystallization. The supply of water (moisture) is essential, especially in the case of addition of chemical agents able to promote the deposition of crystals inside the crack, but “since most infrastructures are exposed to rain or underground water, usually this is an easily satisfiable requirement” [33]. Besides the presence of water, several other variables can affect the phenomenon of self-healing, such as the mix proportions [15], the stress state along the cracks and the steadiness of the cracked state [19] as well as thermal and hygrometric conditions [3, 16]. Moreover, traditional mineral additions for cement replacement, such as fly ash or blast furnace slag, [34, 35] or innovative pozzolanic additions [36, 37], investigated by different researchers, may also promote autogeneous healing because of delayed hydration, since high amounts of these binders remain un-hydrated even at a later age because of the slow pozzolanic reactions or, as in the case of slag, because of latent hydraulicity.

Among the aforementioned proprietary chemical admixtures, special attention has been deserved in recent years to the so-called crystalline admixture, which are a category of Permeability Reducing Admixtures already available and widely employed as such in the construction products market.

Crystalline admixture generally consist of a proprietary mix of active chemicals, carried out in a carrier of cement and sand, which, because of their highly hydrophilic nature, are able to react with water, cement particles but also with the soluble phase of cement hydration products ( $\text{Ca(OH)}_2$ ) and form Calcium Silicate Hydrates and other pore blocking precipitates. These reaction products, on the one hand, increase the density of the CSH phase, and, on the other, deposit in the existing capillaries and micro-cracks activating the self-repairing process. The mechanism is analogous to the formation of CSH and the resulting crystalline deposits become integrally bound with the hydrated cement paste, thus contributing to a significantly increased resistance to water

penetration under pressure. Furthermore, hairline cracks are formed over the life of concrete, and because of that, it would be also desirable that crystalline admixtures store certain “latent” self-healing capacity for further cracks. That capacity would ideally contribute to a recovery of the engineering and mechanical properties of the composite, also as a function of the exposure conditions and durations and of the activated healing mechanisms. Anyway, it is worth remarking that cracks exceeding the self-sealing or self-healing capacity of the concrete may still be developed.

The aforementioned self-healing capacity, though hypothesised through educated guess as above, needs to be systematically investigated. In this paper the results of an experimental investigation performed by the authors will be presented, with reference to the efficacy of crystalline admixtures as promoters of self-healing in both Normal Strength Concrete (NSC) and High Performance Fiber Reinforced Cementitious Composites (HPFRCCs). The methodology employed to characterize the effects of healing, which stands as a key feature of the study, is based on the tailored experimental identification of the recovery of mechanical properties (load bearing capacity, stiffness and, in case of HPFRCCs, ductility and toughness), through which also an indirect assessment of the crack closure could be accomplished.

Moreover, the investigation of the synergy between dispersed fiber reinforcement and self-healing crystalline admixture, which to the authors’ knowledge is herein investigated for the first time, has yielded promising results which are likely to pave the way for future developments to improve the structural efficiency of advanced cement based materials and hence the sustainability of structural and engineering applications made of or retrofitted with them.

## **2. Experimental programme: materials, specimens and tests**

The employed crystalline admixture consists of a blend of cement, sand and microsilica; SEM magnified particles are shown in Figures 1a-b: they have irregular shape and size in the range of about 1-20  $\mu\text{m}$  and their morphology is similar to that of cement grains; EDS analysis confirmed

the presence of calcium, oxygen, silicon, magnesium, aluminium and potassium (Figure 1c). This spectrum is comparable with that of an Ordinary Portland Cement (OPC), except for the slightly higher peak of sulphur.

With reference to the NSC the employed mix design composition is shown in Table 1. Beam specimens, 500 mm long x 100 mm wide x 50 mm thick, were cut from larger slabs (1m x 0.5 m) casted with that mix. After 35 to 42 days curing in a fog room at 20°C and 95% relative humidity, specimens were pre-cracked by means of a COD-controlled 3-point bending set-up (center point loading with a 450 mm span), up to two different levels of residual crack opening (about 130 and 250 µm respectively). Specimens were then either immersed in water at 20°C or exposed to open air, with daily recording of temperature and relative humidity [42]. After scheduled exposure times (1, 3, 6 and 12 months) three point bending tests were performed again on the same specimens according to the same set-up and results between the pre- and post-conditioning response were compared, in order to evaluate, if any, load-bearing capacity and stiffness recovery and calculate related “self-healing indices”.

In the case of HPFRCC, the mix detailed in Table 2 was employed, which, as from previous studies [38-41], because of its self-compacting properties, is likely to exhibit a mechanical performance dependant on the flow-induced fibre alignment. Specimens, similar to the ones described above, except for a 30 mm thickness, were cut from larger slabs, which were casted in such a way that a preferential fibre alignment was obtained. The cutting of the beam specimens,, as schematically sketched in Figure 2, was hence done in such a way that the beam axis was either parallel or orthogonal to the aforementioned direction of preferential alignment of fibres. In comparison with the experimental campaign performed on NSC, the pre-cracking of specimens was performed according to a 4-point bending set-up, under third point loading over a 450 mm span. This was motivated by the need to have a constant bending moment region in the centre of the specimen, throughout which the development of multiple cracking was possible (Figure 3a), as it occurs in the case of a deflection hardening behaviour (Figure 3b), triggered by favourable alignment of fibres

(i.e. parallel to the beam axis). It is worth remarking that in the case of an unfavourable fibre alignment, i.e. orthogonal to the beam axis, one single crack formed, randomly, in the central region of the specimen (Figure 3c), which all exhibit a deflection softening behaviour (Figure 6d). Because of high content of slag in the mix, and of its latent hydraulic activity, specimens were pre-cracked two months after casting, and until then cured in the same fog room environment as above.

In view of the aforementioned behaviour, dependant on the flow induced alignment of fibres, it was decided to pre-crack specimens featuring a deflection softening response (i.e. with fibres perpendicular to the beam axis) up to a COD value equal to 0.5 mm. On the other hand, for specimens with fibres parallel to the axis, most likely featuring a deflection hardening response, three different levels of crack opening were selected and induced in the specimens: two in the pre-peak regime, respectively equal to 1mm and 2 mm, and one in the post-peak regime equal to (COD<sub>peak</sub> + 0.5 mm, COD<sub>peak</sub> = measured value of the COD in correspondence of the peak stress). Because of the stable pre-peak multi-cracking process and of the employed test set-up, the measured value of the COD in the pre-peak regime actually represents the sum of the opening of all the cracks; on the other hand, the value of pre-cracking COD in the post-peak regime has been selected on the basis of an equivalent opening of the unstable localized crack, in analogy to the deflection softening/single cracking case [38,41]. After pre-cracking specimens were immersed in water up to six months.

A synopsis of the whole experimental programme is provided in Tables 3 and 4. More details can be found in [27,42-44].

### **3. Experimental results: analysis and discussion**

#### **3.1 *Normal Strength Concrete***

In Figure 4 the results of a typical test, in terms of nominal stress  $\sigma_N$  vs. COD curves, are shown: the graphs are built up to compare the curves pertaining respectively to the pre-cracking test and to



the post-conditioning up-to-failure test for the same specimens.

From the values of nominal bending stresses and flexural stiffness, as denoted in Figure 4, an Index of Stress Recovery (ISR) has been defined and calculated as follows:

$$ISR = \frac{P_{\max \text{ reloading}} - P_{\text{unloading}}}{P_{\max, \text{uncracked}} - P_{\text{unloading}}} \quad (1)$$

Figure 5 shows the trend of the Indices of Stress Recovery vs. the exposure time for different exposure conditions. The following remarks hold:

- specimens immersed in water and made with concrete containing the crystalline additive exhibited an almost immediate and quite significant recovery, which even upon prolonged exposure, e.g. after six and up to twelve months, showed continuing improvement of the recovered performance; on the other hand specimens made with plain concrete and immersed in water showed a more gradual recovery, which anyway, even after six months, barely attained half the level achieved by concrete with the crystalline additive;
- specimens exposed to open air and made with concrete containing the crystalline additive showed a gradual recovery capacity, as high as the one exhibited by plain concrete specimens immersed in water; on the contrary a scant recovery capacity at all was exhibited by specimens without the additive (maximum 5% after twelve months).

Pictures obtained by stereo-microscope in Figures 6 a-d and with SEM and related EDS analysis in Figures 7 a-b confirm the aforementioned statements and are as well coherent with the analysed EDS spectrum of the admixture as shown in Figure 1c.

From the nominal bending stress  $\sigma_N$  vs. COD curves an estimation of the crack closure due to the self-healing can be provided. The proposed methodology (Figure 8a) consists in operating a “backward” shifting along the COD axis, of the stress-COD curve representative of the behaviour of each pre-cracked specimen after environment conditioning, until the stress-COD curve of the same specimen, as measured during the pre-cracking test on the virgin undamaged sample is met. The new value of the “origin” COD can be estimated by drawing, from the aforementioned point on

the curve of the virgin sample, an unloading branch with a slope equal to that of the closest unloading previously measured on the virgin sample itself. This allows to define and calculate an Index of Crack Healing:

$$\text{ICH}_{\text{stress-crack opening}} = \frac{\text{COD}_{\text{pre-cracking}} - \text{COD}_{\text{post-conditioning}}}{\text{COD}_{\text{pre-cracking}}} \quad (2)$$

From the trends of ICH vs. immersion time (Figure 9), the following remarks to be highlighted:

- a remarkable crack closure may occur, since from the beginning of the surveyed exposure times, for specimens containing the crystalline additive and immersed in water; the same specimens, when exposed to air, show a slower recovery capacity;
- immersion in water triggers the self healing also for specimens without any additive, but at a much slower pace: only after 2 to 3 months effects start being visible and after 6 months a performance comparable to specimens with the additive was achieved; specimens without any additive exposed to air hardly show any appreciable recovery and only after prolonged exposure a moderate crack closure starts appearing.

The trends of Index of Stress Recovery vs. the related crack healing indices allow an insightful synopsis to be provided about the investigated phenomena as well as a preliminary methodological quantification to be attempted. Effects of exposure conditions and of the crystalline additive are evident. In detail, some load bearing capacity is recovered even for very low values of estimated crack healing, with a more moderate influence of the additive, also considering the narrow data range provided by experiments. A better understanding could be achieved through a dedicated analysis of the strength development of crack healing products, as also affected by exposure conditions, which has been regarded as out of the scope of this work.

### **3.2 High Performance Fibre Reinforced Cementitious Composites**

The results of pre-cracking and post-conditioning 3-point bending tests performed on specimens featuring a deflection softening behaviour, because of an unfavourable alignment of the fibres to the

direction of the applied bending stress, are shown in Figures 11 a to c.

Specimens without the crystalline admixture featured some recovery of the post-cracking stress bearing capacity, as witnessed by the new “cracking peak” detected in post-immersion tests, followed by a gradual release of the stress. This can be evidently attributed to a quite strong re-establishment of “mechanical connections” between the two faces of the crack, due to the delayed hydration of anhydrous binder particles and the consequent formation of new hydration products, which are likely to feature a high compatibility with the old material. Specimens with the crystalline admixture exhibited a higher recovery of the load bearing capacity, with new cracking strength even higher than the one exhibited by the virgin specimen. This continuous healing has even led, after six months, to achieve some kind of post-conditioning deflection hardening behaviour. In both cases, a moderate improvement of the healing capacity upon immersion time was detected.

In the case of a deflection hardening behaviour, an immediate “visual” appreciation of the self healing capacity can be consistently performed if for each specimen both the nominal stress and the COD are plot dimensionless to the COD and nominal bending stress value at which unloading occurred in the pre-cracking stage (if the pre-cracking value of the COD was in the pre-peak regime) or to their peak values ( $COD_{peak} - \sigma_{N,peak}$ ), in case the pre-cracking value of the COD was beyond the peak (Figures 12 a to c). The results obtained confirm the aforementioned statements, with reference to the difference between specimens without and with the additive. A huge recovery of load bearing capacity has been detected in the latter case, which is, in relative terms, significantly higher also with reference to the case of deflection softening specimens.

This may lead to hypothesize that, because of the somewhat expansive reaction provided by the crystalline admixture reactions, some sort of “internal chemical pre-stressing” of fibres may have occurred, enhanced by the favourable alignment of fibres with respect to the applied stress. Such a concept was already addressed in the early 60s by Klein et al. [45] as well as by Lin and Klein [46], who used expansive cements in reinforced concrete elements, and is likely to be greatly exploitable through the synergistic combination of a dispersed fibre reinforcement and admixture featuring

expansive reactions, like the crystalline ones employed in this study. The multiple cracking has also favoured such an effect to be evenly distributed throughout the specimen, thus leading to a more remarkable recovery of the performance than what obtained in the case of deflection softening specimens (or deflection hardening specimens pre-cracked beyond the peak), where it was (mainly) concentrated into a single localized crack.

From the experimental results the Index of Stress Recovery has been defined in order to quantify the effects of the crack healing on the mechanical performance of the material.

For deflection softening and deflection-hardening specimens pre-cracked beyond the peak:

$$\text{Index of stress recovery ISR} = \frac{f_{peak, post\text{-}conditioning} - \sigma_{N\text{ unloading pre-cracking}}}{f_{peak, pre-cracking} - \sigma_{N\text{ unloading pre-cracking}}} \quad (3a)$$

For deflection hardening specimens pre-cracked before the peak:

$$\text{Index of stress recovery ISR} = \frac{(f_{peak, post\text{-}conditioning} - \sigma_{N\text{ unloading pre-crack}})}{(f_{peak, virgin} - \sigma_{N, unloading, virgin})} \frac{\sigma_{N, unloading, virgin}}{\sigma_{N, unloading pre-crack}} - 1 \quad (3b)$$

Notation and significance of Indices are shown in Figure 13 a to c.

Plots in Figure 14 a, referring to deflection softening specimens, and in Figure 14 b, for deflection hardening specimens, confirm the statements exposed above, mainly with reference to the effect of the crystalline admixture in promoting a complete healing of the cracks, even in the case of higher damage. Specimens with larger crack openings, in the pre-peak regime, and containing the crystalline admixture exhibited a dramatic recovery of the load bearing capacity, which furthermore increased upon prolonged exposure time. The aforementioned “internal pre-stressing” effect can be called to explain it: the larger the cracks, the higher the amount of reactive particles coming into contact with water. Specimens pre-cracked beyond the peak coherently exhibited a lower recovery.

The confirmation that the measured recovery of the material performance is due to crack healing, and hence an indirect assessment of the guessed chemical pre-stressing action produced by the admixture, has been obtained through Ultrasonic Pulse Velocity (UPV) tests, performed according to the set-up shown in Figure 15a-b. In Figures 15 c-d the values of the velocities are plotted, as

measured in the central and edge portion of the specimen respectively, and in the three aforementioned testing stages, i.e. before pre-cracking, after pre-cracking and after conditioning.

It can be immediately observed that, for the data referring to the central part of the specimen, which undergoes cracking, a significantly slower wave is detected after cracking, followed, in case and as a function of the crack-opening and exposure conditions and durations, by recovery in the post-conditioning stage. On the other hand for the data referring to the edge portion of the specimen, no relevant change is detected neither between before and after pre-cracking, nor, more significantly, between after pre-cracking and after conditioning tests. Once again the effect of the admixture clearly appears in promoting a more solid recovery.

Through processing of digital optical microscope pictures, garnered at different magnifications (x50 and x200) before and after healing, performed with software Adobe Photoshop CS6, the evolution of crack width, as affected by healing, was measured. It is worth remarking that for deflection softening specimens and deflection hardening specimens pre-cracked in the post-peak regime only one crack had to be measured, which is the single crack or the crack unstably localizing after the peak respectively. On the other hand, for deflection hardening specimens pre-cracked in the pre-peak regime all multiple formed cracks were monitored and the measures have been then averaged. Reference was made to the  $w_{avg}$ , *average crack width*, obtained by averaging the crack width measured at three fixed positions (approximately located 10 mm from the edges of the pictograph and at mid-length of the surveyed portion of the crack - Figure 16) [47]. From the values of crack-opening, measured as above both in the pre-cracking and in the post-conditioning regime an Index of Crack Healing was defined, as from Equation (2).

Evolution of Index of Crack Healing over time (Figure 17) confirm the aforesaid statements with reference to the efficacy of the synergy between crystalline admixture and dispersed fibre reinforcement in enforcing, though the expansive action of healing products, a chemical pre-stressing which resulted in a far larger improvement of the mechanical performance of the material than what obtained with mere autogenous healing.

Visual confirmation of the healed cracks and correlation with the different calculated indices of recovery of mechanical properties and crack closure can be clearly appreciated from sample pictures shown in Figure 18 a-c. Fibers crossing the healing cracks also performed as sites for deposition of healing products (Figure 19), as also observed by other authors with reference to, e.g, synthetic fibers [48]. Healing products, completely enveloping the fibers, were also likely to delay and/or stop any corrosion, which might have occurred because of their direct contact with water. The measured recovery of mechanical performance leads to argue that the healing is able to overcome any detrimental effect resulting from the initiation of the aforementioned fiber corrosion, which is in any case limited only to the fibers crossing the crack.

This is also confirmed by the SEM analyses of the fractured healed surfaces in specimens both without and with the crystalline admixture. In the latter case a rather amorphous structure of the products covering the aggregate grains is observed (Figure 20a) with typical composition of cement hydration products (Figure 20b), thus confirming that healing is mainly due to delayed hydration of unhydrated binder particles. In the former, the presence of crystals is observed (Figure 20c) with chemical composition (Figure 20d) compatible with the composition of the admixture. Deposition of healing products on the surface of the fibers is also evident (Figure 20e). The observed rupture of the fiber is attributable to an improved bond rightly resulting from the deposition of the aforementioned products, confirming the hypothesis about chemical pre-stressing resulting from the admixture action as highlighted above.

#### **4. Concluding remarks**

The effects of crystalline admixtures as catalysts of self-healing in cement-based materials have been investigated, with reference to a Normal Strength Concrete and to a High Performance Fiber Reinforced Cementitious Composite. A methodology has been conceived and validated to measure and quantify the effects of self-healing on the mechanical properties of cement-based materials, in terms of load bearing capacity, stiffness and, for deflection hardening fiber reinforced concrete, also

in terms of deformation capacity. The methodology is based on pre-cracking beam specimens to prescribed crack-widths, exposing them to suitable environmental conditioning (water immersion has been considered in this paper), and, after that, testing them again until failure according to the same set-up employed for pre-cracking. Self-healing capacity has been evaluated by seeking suitable matching between the load-crack opening curves obtained for the virgin specimen and for the conditioned one. The consistency of the obtained data, despite some scattering due to the wide variety of investigated variables, is a solid proof of the reliability of the proposed methodology.

Both in the case of NSC and HPFRCC, the crystalline admixture enhances and makes more reliable the autogenous healing capacity of cementitious composites. This, in the case of HPFRCC can be quite significant, because of high binder content and low w/b ratio and hence of likeliness of delayed hydration reactions. Moreover, in the case of HPFRCCs, the measured performance of the healed material containing crystalline admixture, can result significantly better than the one of virgin specimens: it can be argued that some kind of internal “chemical pre-stressing” of fibres may be triggered by the expansive reactions of the admixtures, which needs anyway to be further and more systematically investigated.

In almost all the investigated experimental situations, with the presence of crystalline admixture, the largest part of the recovery of mechanical performance occurred after short exposure time (1 month). Anyway the fact that the recovery continued, even if with a slower trend, also upon prolonged exposure time, is likely to be a guarantee about the long term effectiveness and repeatability of the healing phenomena, in view of the fact that new “healing-needing” cracks may form along time, at locations other than the first crack one. In this framework, the long-term performance and repeatability of the healing capacity, including effects of sustained through-crack stresses, stands as the major research need which has to be urgently addressed to spread this self-healing technique into the construction market.

## **Acknowledgements**

The authors thank Mr. Robert Revera and dr. Chris Chen, Penetron Intl. Ltd. and MArch. Enrico Maria Gastaldo Brac, Penetron Italia Ltd. for their enthusiastic support in this research. The support of the Young Researchers grant 2011- Politecnico di Milano is also gratefully acknowledged.

## **References**

- [1] Mihashi, H and Nishiwaki, T. Development of engineered self-healing and self-repairing concrete. State-of-art report. J. Adv. Concr. Techn. 2010; 10; 170-184.
- [2] Tittelboom, K.V. and De Belie, N. Self-healing in cementitious materials – A review. Materials, 2013; 6,; 2182-2217.
- [3] Lauer, K.R. and Slate, F.O. Autogeneous healing of cement paste. ACI J. 1956; 52 (6); 1083-1097.
- [4] Bertolini, L., Elsener, B., Pedferri, P., Polder, R. Corrosion of steel in concrete: prevention, diagnosis, repair. Weinheim, Wiley VCH, 2003.
- [5] Abrams, D.A. Tests of bond between concrete and steel. University of Illinois, 1913; Bulletin 71, 107 pp.
- [6] Loving, M.W. Autogenous healing of concrete. American Concrete Pipe Association. 1936, Bulletin 13.
- [7] Ramm, W. and Biscopig, M. Autogeneous healing and reinforcement corrosion of water-penetrated separation cracks in reinforced concrete. Nucl. Eng. & Des. 1998; 179; 191-200.
- [8] Hearn, N. and Morley, C.T. Self-Sealing Property of Concrete: Experimental Evidence. Mats. & Structs. 1997; 30; 404-411.
- [9] Neville, A. Autogenous Healing: a concrete miracle?, Concr. Intl. 2002; 24; 76-82.



- [10] Turner, L. The autogenous healing of cement and concrete: its relation to vibrated concrete and cracked concrete. Intl. Ass. Test. Mats. 1937, London Congress; 344.
- [11] Whitehurst, E.A. Soniscope tests concrete structures. ACI J., 1951; 47; 433-444.
- [12] Hearn N. Self-Sealing, Autogenous Healing and Continued Hydration: What is the Difference?, Mats. & Structs. 1998; 31; 563-567.
- [13] Edvardsen, C. Water Permeability and Autogenous Healing of Cracks in Concrete. ACI Mat. J. 1999; 96; 448-454.
- [14] Aldea, C.M., Song, W.J. and Popovics, J.S. Extent of Healing of Cracked Normal Strength Concrete, ASCE J. of Mats. in Civ. Engrg. 2000; 2; 92-96.
- [15] Dhir, R.K., Sangha C.M. and Munday J.G. Strength and Deformation Properties of Autogenously Healed Mortars. ACI J. 1973; 70; 231-236.
- [16] Reinhardt, H.W. and Jooss, M. Permeability and self-healing of cracked concrete as a function of temperature and crack width. Cem. Concr. Res., 2003; 33: 981-985.
- [17] Jacobsen, S., Sellevold, E.J. Self healing of high strength concrete after deterioration by freeze/thaw, Cem. Concr. Res., 1993; 26: 55-62.
- [18] Sahmaran, M., Keskin, S.B., Ozerkan, G., Yaman, I.O. Self healing of mechanically loaded self consolidating concretes with high volumes of fly ash, Cem. Concr. Compos., 2008; 30: 872-879.
- [19] Ngab, A.S., Nilson A.H. and Slate, F.O. Shrinkage and creep of high strength concrete. ACI J. 1981; 78; 225-261.
- [20] Hannant, D.J. and Keer, J.G. Autogenous healing of thin cement based sheets. Cem. Concr. Res. 1983; 13; 357-365.
- [21] Grey, D.J. Autogenous healing of fiber/matrix interfacial bond in fiber reinforced mortar.

Cem. Concr. Res. 1984; 14; 315-317.

[22] Yang, Y., Lepech, M.D., Yang, E.H. and Li, V.C.. Autogenous healing of Engineered Cementitious Composites under wet-dry cycles: Cem. Concr. Res. 2009; 39; 382-390.

[23] Qian, S., Zhou, J., de Rooji, M.R, Schlangen, E., Ye, G. and van Breugel, K. Self-healing behavior of strain hardening cementitious composites incorporating local waste materials, Cem. Concr. Compos., 2009, 31, 613-621.

[24] Qian, S.Z., Zhou, J. and Schlangen, E. Influence of curing condition and precracking time on the self-healing behavior of Engineered Cementitious Composites, Cem Concr. Compos., 2010, 32, 686-693.

[25] Yang, Y., Yang, E.H. and Li, V.C. Autogeneous healing of engineered cementitious composites at early age, Cem. Concr. Res., 2011, 41, 176-183.

[26] Li, M. and Li, V.C. Cracking and healing of engineered cementitious composites under chloride environment, ACI Mat. J., 2011, 108, 333-340.

[27] Ferrara, L., Ferreira, S.R., Krelani, V., Silva, F. and Toledo Filho, R.D.: "Effect of natural fibres on the self healing capacity of high performance fibre reinforced cementitious composites", Proceedings SHCC3, 3rd international RILEM conference on strain hardening cementitious composites, Dordrecht, The Netherlands, November 3-5, 2014, pp. 9-16.

[28] Mihashi, H., Ahmed, S.F.U. and Kobayakawa, A. Corrosion of reinforcing steel in Fiber Reinforced Cementitious Composites. J. Adv. Concr. Technol. 2011; 9; 159-167.

[29] Jonkers, H.M. Bacteria based self-healing concrete. Heron, 2010; 56 (1/2); 1-12.

[30] Snoeck, D., van Tittelboom, K., Steuperart, S., Dubruel, P. and de Belie, N. Self-healing cementitious materials by the combination of microfibers and superabsorbent polymers, J. of Intell. Mat. Syst. and Struct., 2014, 25, 13-24.

- [31] Van Tittelboom, K., De Belie, N., Van Loo, D. and Jacobs, P. Self-healing efficiency of cementitious materials containing tubular capsules filled with healing agent, *Cem. Concr. Compos.*, 2011, 33, 497-505.
- [32] Yang, Z., Hollar, J., He, X. and Shi, X. A self-healing cementitious composite using oil/core silica gel shell microcapsules, *Cem. Concr. Compos.*, 2011, 33, 506-512.
- [33] ACI 212-3R-10. Report on chemical admixtures for concrete. 2010, 61pp.
- [34] Termkhajornkit, P., Nawa, T., Yamashiro, Y. and Saito, T. Self healing ability of fly ash-cement systems. *Cem. Concr. Compos.*, 2009; 31; 195-203.
- [35] Sisomphon, K. and Copuroglu, O. Self healing mortars by using different cementitious materials, in *Proc. Intl. Conf. on Advances in construction materials through science and engineering*, Hong Kong, China, 5-7 September 2011.
- [36] Carsana, M., Frassoni, M., Bertolini, L. Comparison of ground-waste-glass with other supplementary cementitious materials, *Cem. Concr. Compos.*, 2014, 45, 39-45.
- [37] Bertolini, L., Carsana, M., Frassoni, M. and Gelli, M. Pozzolanic additions for durability of concrete structures, *Constr. Mater.*, ICE, 2011, 164; 283-291.
- [38] Ferrara, L., Ozyurt, N. and di Prisco, M., High mechanical performance of fiber reinforced cementitious composites: the role of “casting-flow” induced fiber orientation, *Mats. & Struct.*, 2011, 44; 109-128.
- [39] Ferrara, L., Faifer, M. and Toscani, S., A magnetic method for non destructive monitoring of fiber dispersion and orientation in Steel Fiber Reinforced Cementitious Composites – part 1: method calibration, *Mats. & Struct.*, 2012, 45; 575-589.
- [40] Ferrara, L., Faifer, M., Muhaxheri, M. and Toscani, S., A magnetic method for non destructive monitoring of fiber dispersion and orientation in Steel Fiber Reinforced Cementitious

- Composites – part 2: correlation to tensile fracture toughness, *Mats. & Structs.*, 2012, 45; 591-598.
- [41] di Prisco, M., Ferrara, L. and Lamperti, M.G.L., Double Edge Wedge Splitting (DEWS): an indirect tension test to identify post-cracking behaviour of fibre reinforced cementitious composites, *Mats. & Structs.*, 2013, 46;1893-1918.
- [42] Ferrara, L., Krelani, V. and Carsana, M., A fracture testing based approach to assess crack healing of concrete with and without crystalline admixtures, *Constr. Build. Mats.*, 2014, 68; 515-531.
- [43] Ferrara, L., Krelani, V., Moretti, F., Roig Flores, M. and Serna Ros, P., Effects of autogenous healing on the recovery of mechanical performance of High Performance Fibre Reinforced Cementitious Composites (HPFRCCs): part 1, submitted for publication to *Cement and Concrete Composites*, December 13, 2015.
- [44] Ferrara, L., Krelani, V. and Moretti, F., Autogenous healing on the recovery of mechanical performance of High Performance Fibre Reinforced Cementitious Composites (HPFRCCs): part 2 – correlation between healing of mechanical performance and crack sealing, submitted for publication to *Cement and Concrete Composites*, December 23, 2015.
- [45] Klein, A., Karby, T. and Polivka, M., Properties of expansive cement for chemical prestressing, *ACI J.*, 1961, 58; 59-82;
- [46] Lin, T.Y. and Klein, A., Chemical prestressing of concrete elements using expansive cements, *ACI J.*, 1963, 60; 1187-1218.
- [47] Roig-Flores, M., Moscato, S., Serna. P. and Ferrara, L., Self-healing capability of concrete with crystalline admixtures in different environments, *Constr. Build. Mats.*, 2015, 86; 1-11.
- [48] Snoeck, D. and de Belie, N., Repeated Autogenous Healing in Strain-Hardening Cementitious Composites by Using Superabsorbent Polymers, *ASCE J. Mat. Civ. Engrg.*, 2016, 28.

## Tables

**Table 1.** Mix composition of investigated NSCs.

Constituent	W/out additive	With additive
Cement type II 42.5	300	300
Water	190	190
Superplasticizer (lt/m <sup>3</sup> )	3	3
Fine aggregate 0-4 mm	1078	1080
Coarse aggregate 4-16 mm	880	880
Crystalline admixture	=	3

**Table 2.** Mix composition of investigated HPFRCCs

Constituent	W/out additive	With additive
Cement type I 52.5	600	600
Slag	500	500
Water	200	200
Superplasticizer (lt/m <sup>3</sup> )	33	33
Fine aggregate 0-2 mm	982	982
Straight steel fibres $l_f/d_f = 13/0.16$	100	100
Crystalline admixture	=	3

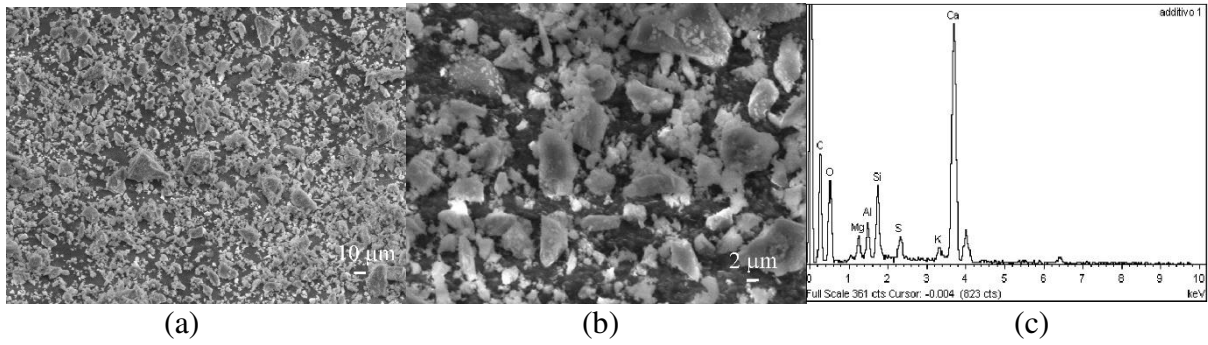
**Table 3.** Synopsis of experimental programme for NSC

	Water immersion					Air exposure				
	1m	2m	3m	6m	12m	1m	2m	3m	6m	12m
<b>With crystalline admixture</b>										
<i>Uncracked</i>	1	2	2	2	2	1	2	2	2	2
<i>Precracked 200 <math>\mu</math>m</i>	1	2	2	2	2	1	2	2	2	2
<b>Without crystalline admixture</b>										
<i>uncracked</i>	1	2	2	2	2	1	2	2	2	2
<i>Precracked 200 <math>\mu</math>m</i>	1	2	2	2	2	1	2	2	2	2

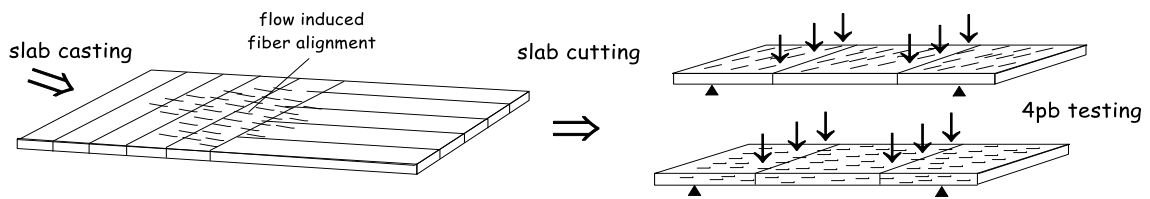
**Table 4.** Synopsis of experimental programme for HPFRCC

Pre-crack opening		Defl. softening			Deflection hardening								
		0.5 mm			1 mm	2 mm	COD <sub>peak+0.5mm</sub>						
		Exposure duration (months)											
Pre-crack age		1	3	6	1	3	6	1	3	6	1	3	6
w/out admixture	2 months	3	2	3	1	1		1	1	1	1	1	1
with admixture	2 months	3	3	3	1	1	1	1	2	3	1	2	1

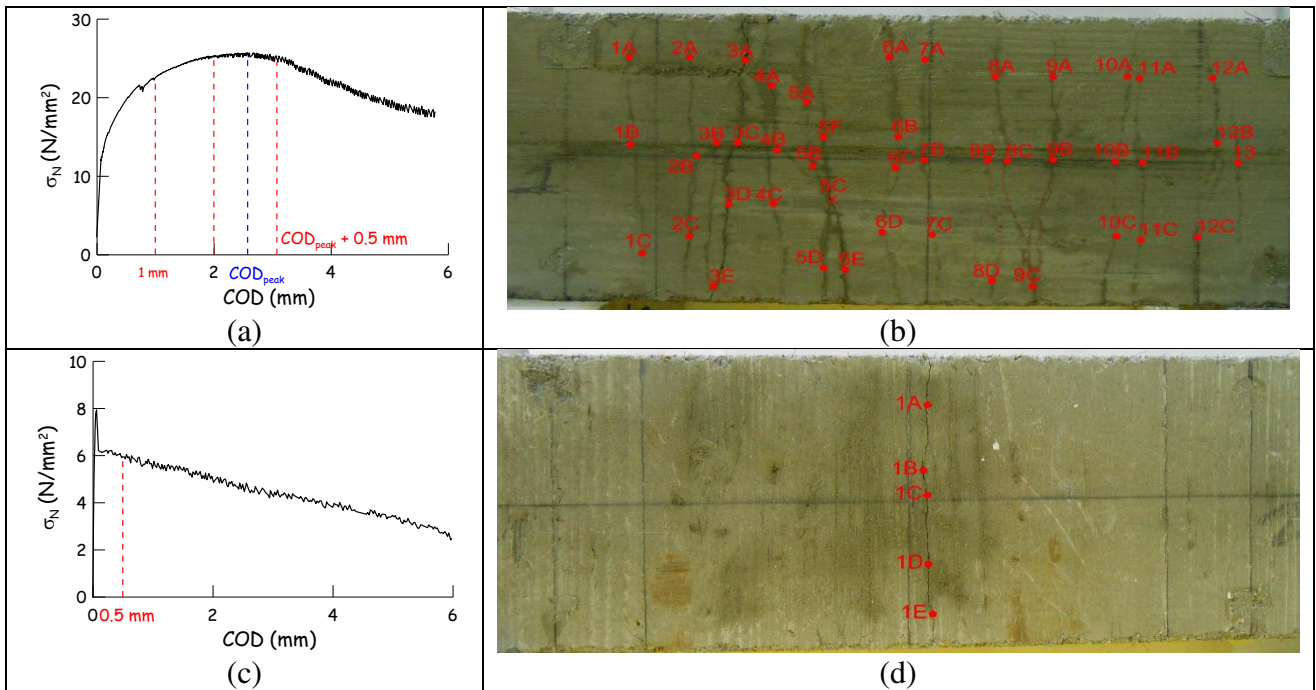
## Figures



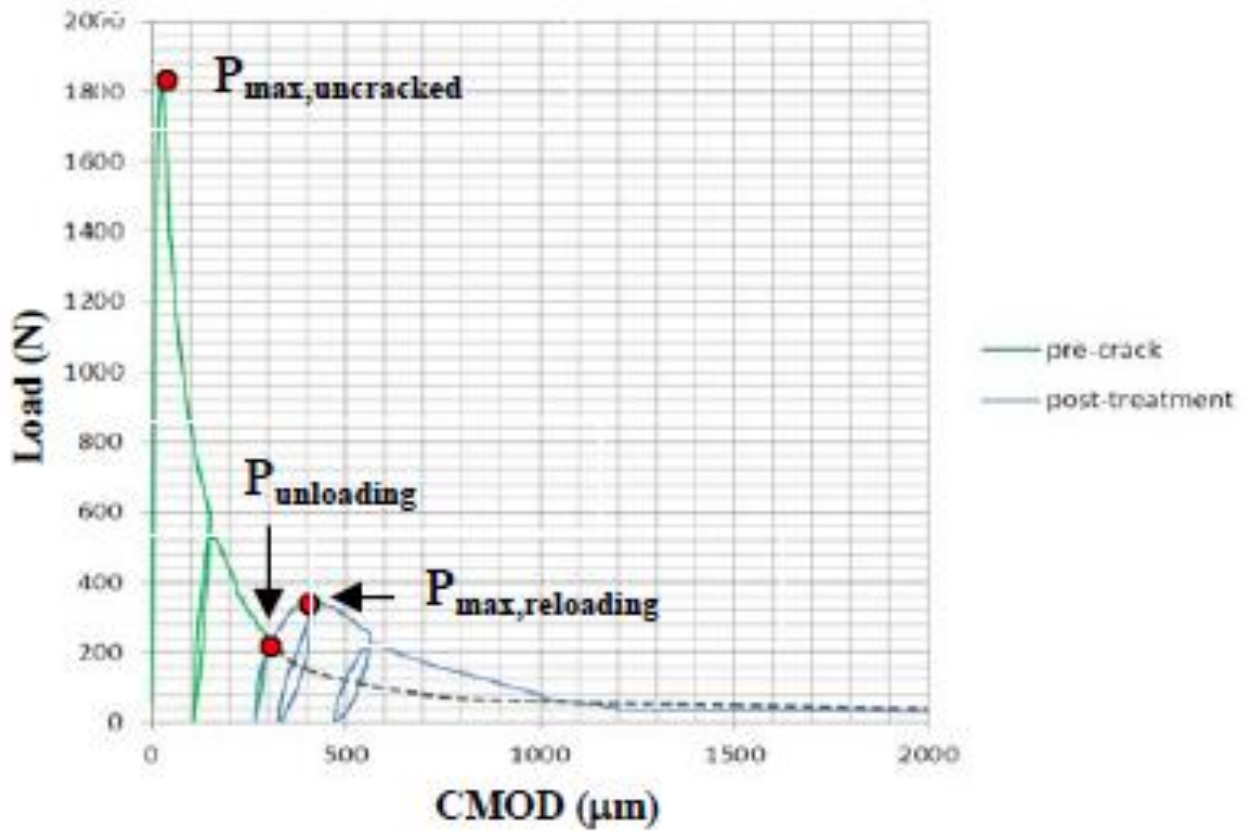
**Figure 1:** SEM magnification (a,b) and EDS analysis (c) of admixture particles.



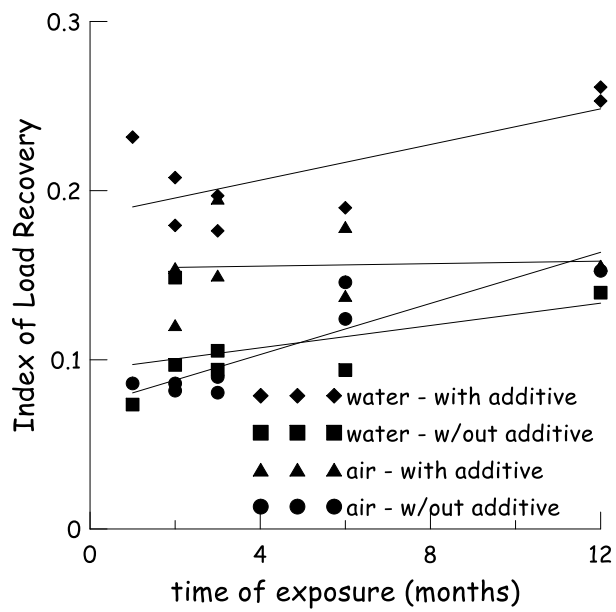
**Figure 2:** HPFRCC slab casting scheme and beam specimen cutting and testing procedure.



**Figure 3:** nominal stress  $\sigma_N$  vs. COD curves and crack patterns for specimens featuring: (a-c) stable pre-peak multi-cracking and deflection hardening behavior (fibers parallel to the beam axis); (b-d) unstable crack localization and deflection softening behavior (fibers orthogonal to the beam axis).



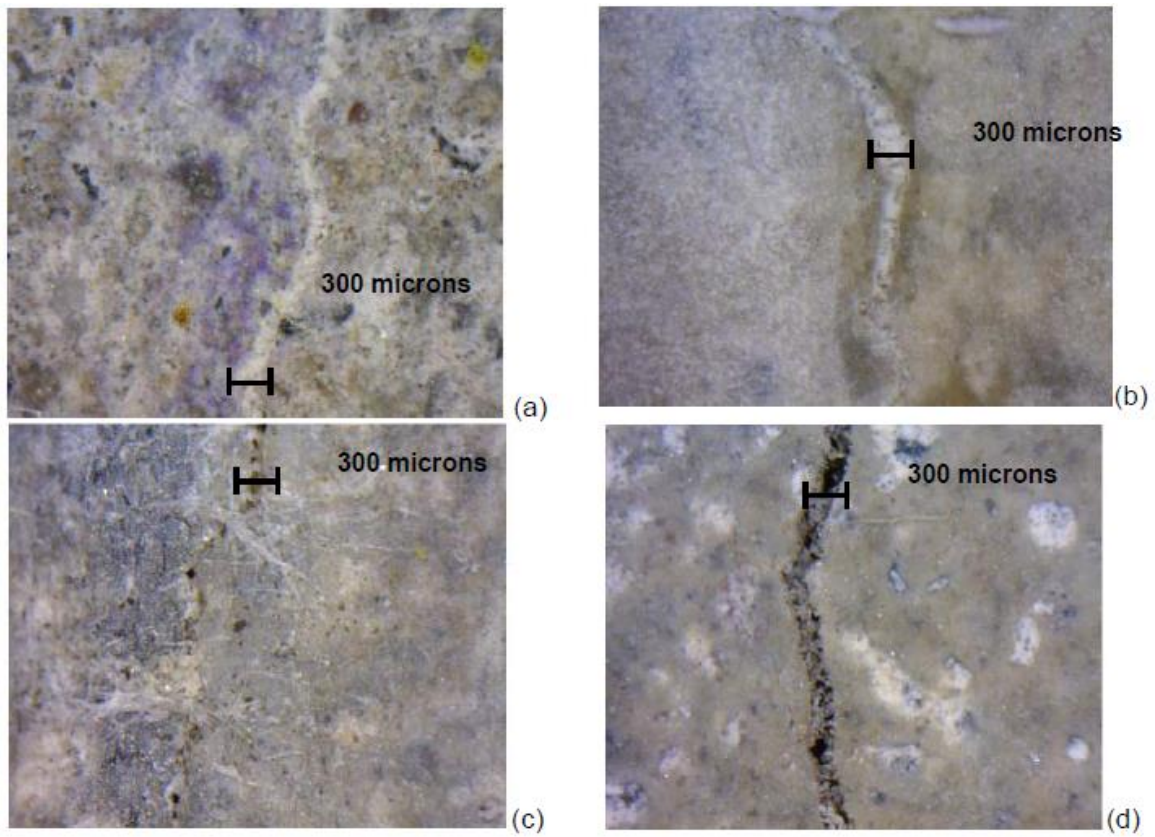
**Figure 4:** Example of stress vs. COD curves for specimens submitted to pre-cracking and post-conditioning 3pb tests.



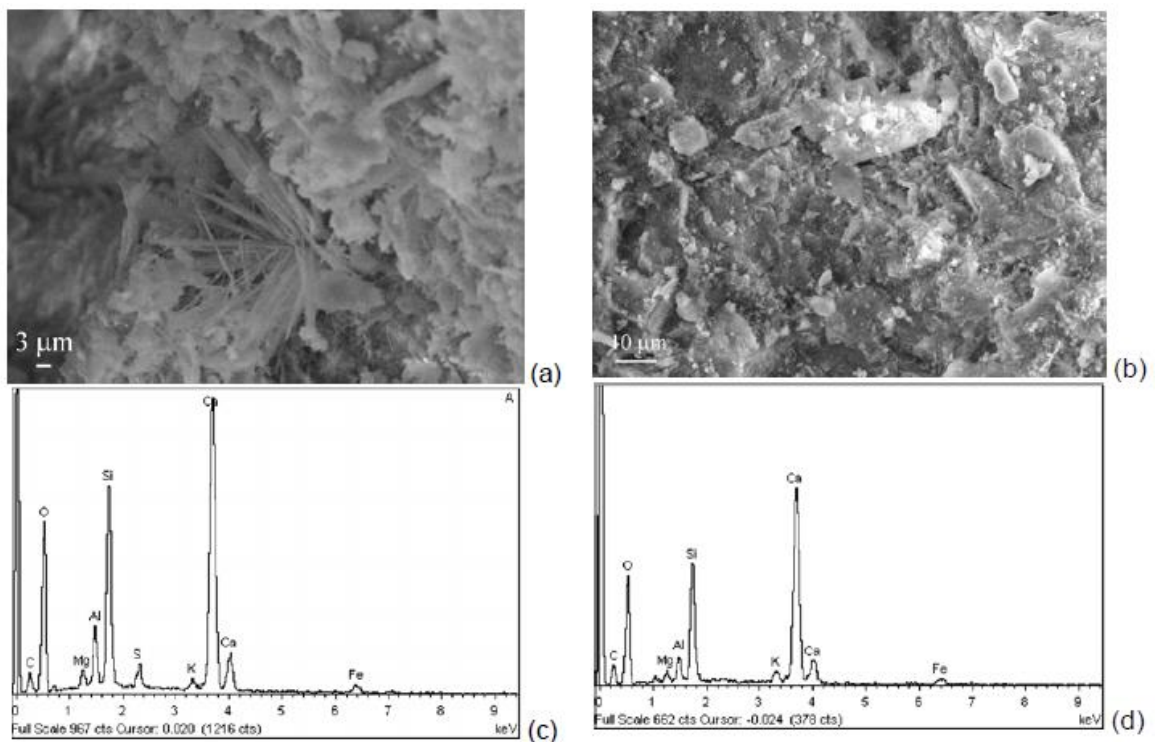
(a)

(b)

**Figure 5:** Indices of Stress Recovery vs. exposure time.

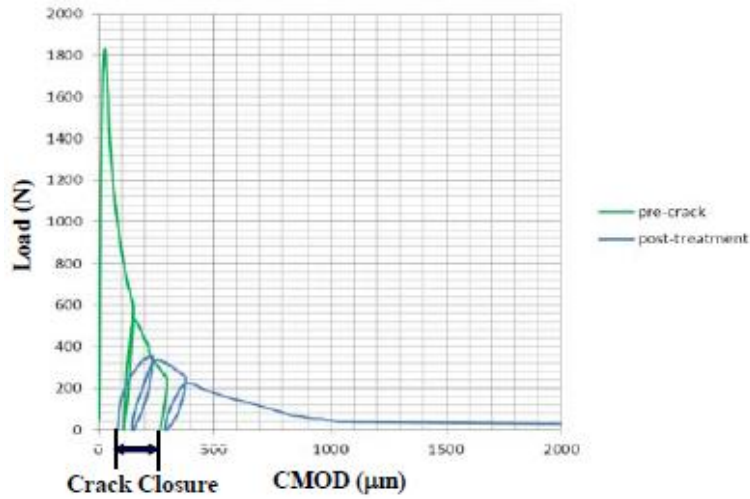


**Figure 6:** healed/healing cracks for specimens with (a,c) and without (b,c) crystalline additive after six months of immersion in water (a,b) and exposure to air (c,d).

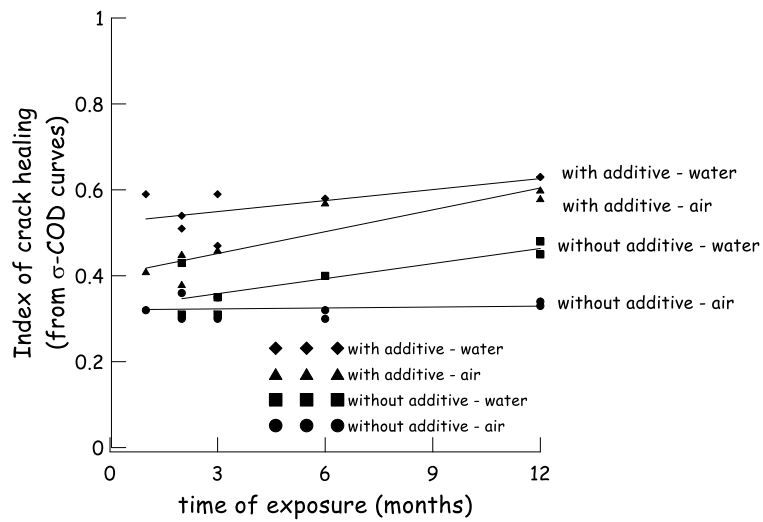


**Figure 7:** SEM images and EDS analyses for specimens with (a,c) and without (b,c) crystalline additive after three months of immersion in water.

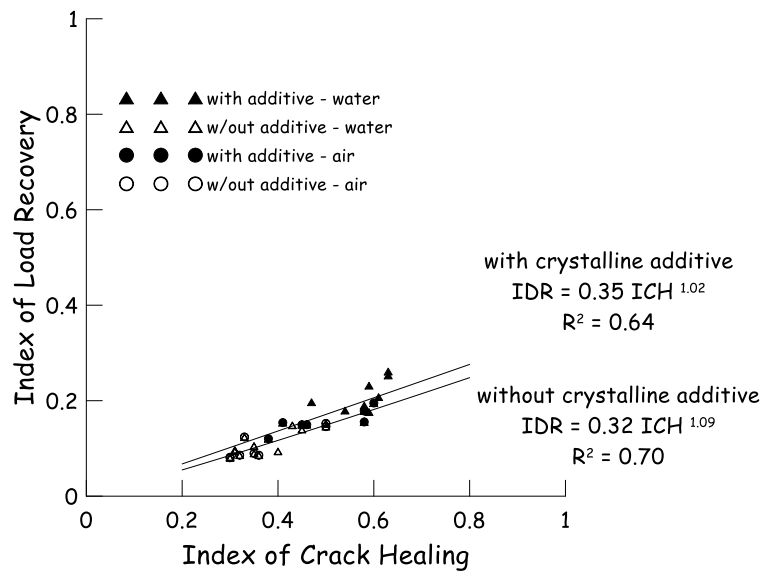




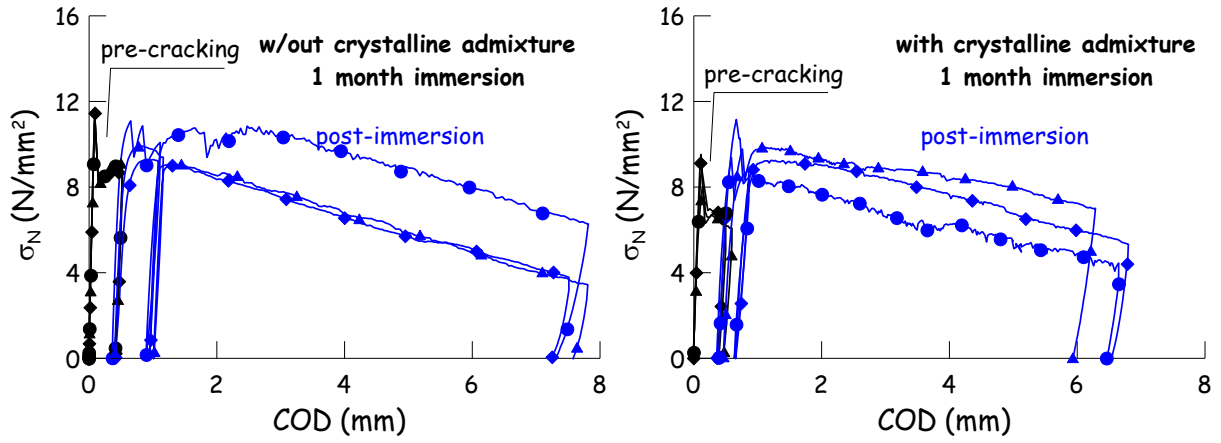
**Figure 8:** Graphical explanation of the procedure to estimate crack closure from  $\sigma_N$ -COD curves



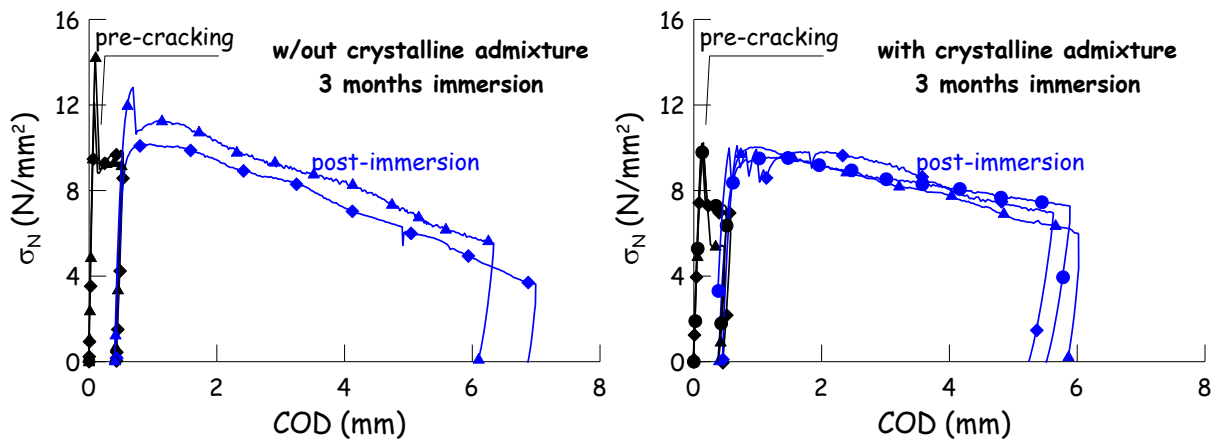
**Figure 9:** Index of Crack Healing (as evaluated from  $\sigma_N$ -COD curves) vs. exposure time.



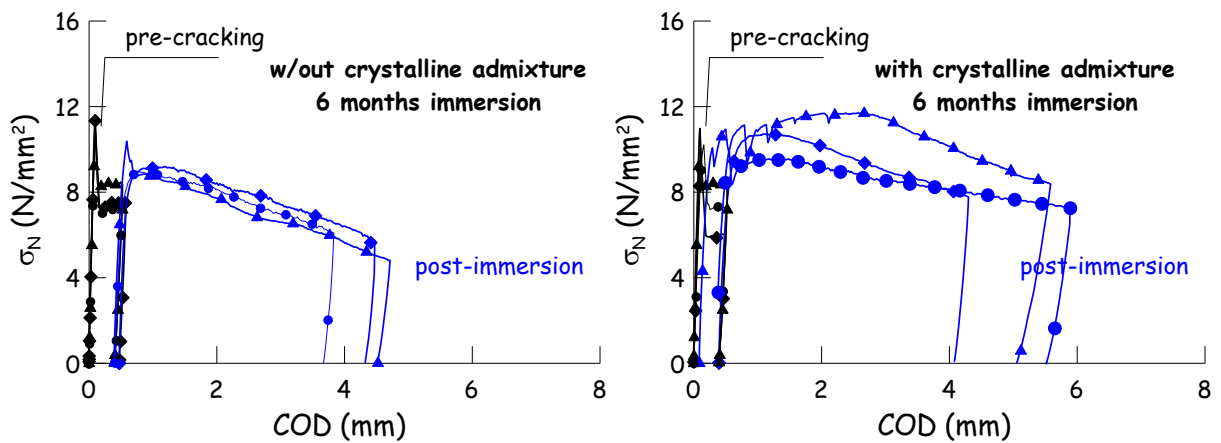
**Figure 10:** Index of Load Recovery vs. Index of Crack Healing.



(a)

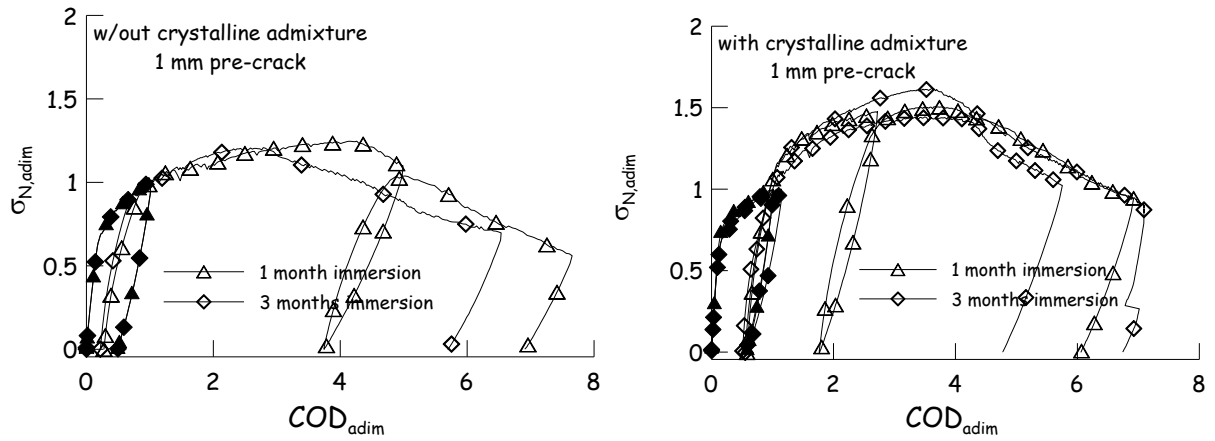


(b)

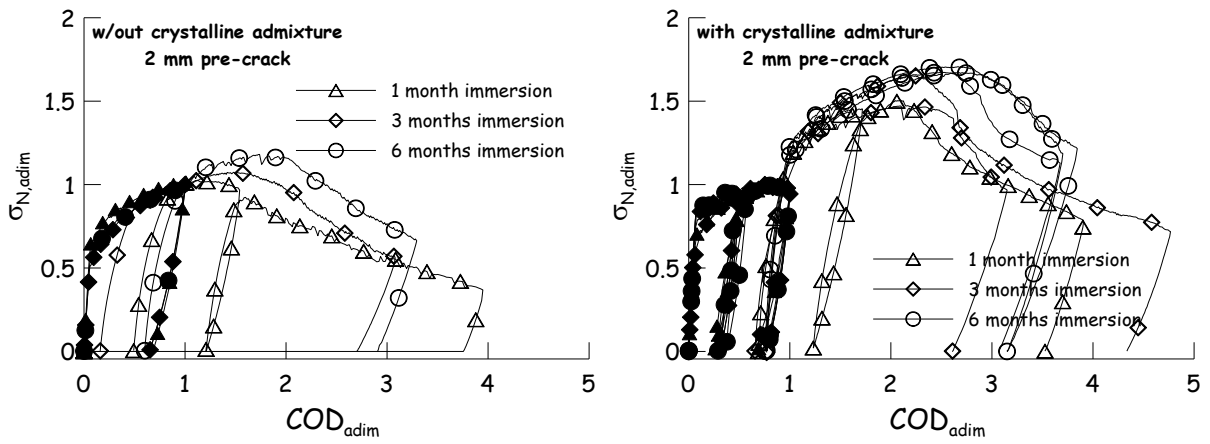


(c)

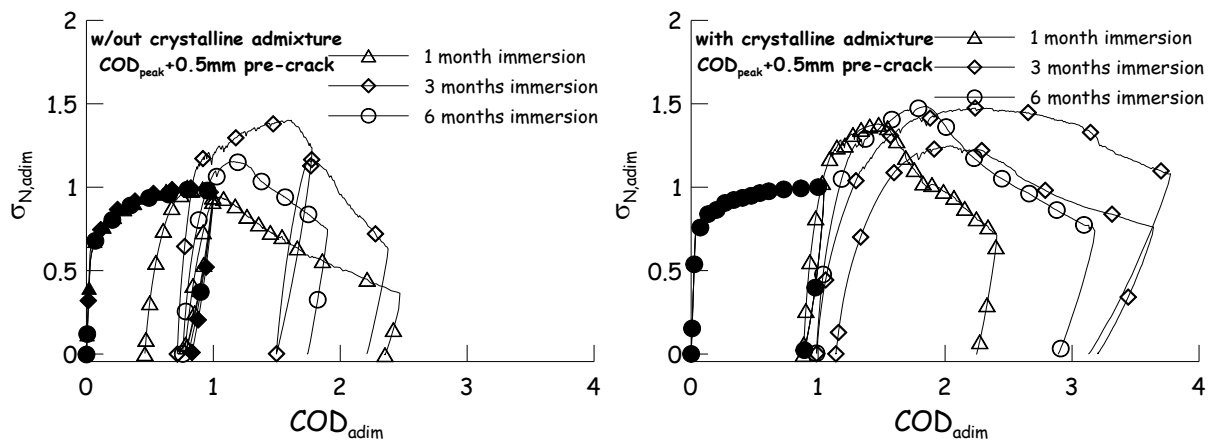
**Figure 11:**  $\sigma_N$  vs. COD response of deflection softening specimens without and with the crystalline admixture pre-cracked at 0.5 mm and after 1 (a) 3 (b) and 6 months (c) immersion in water.



(a)

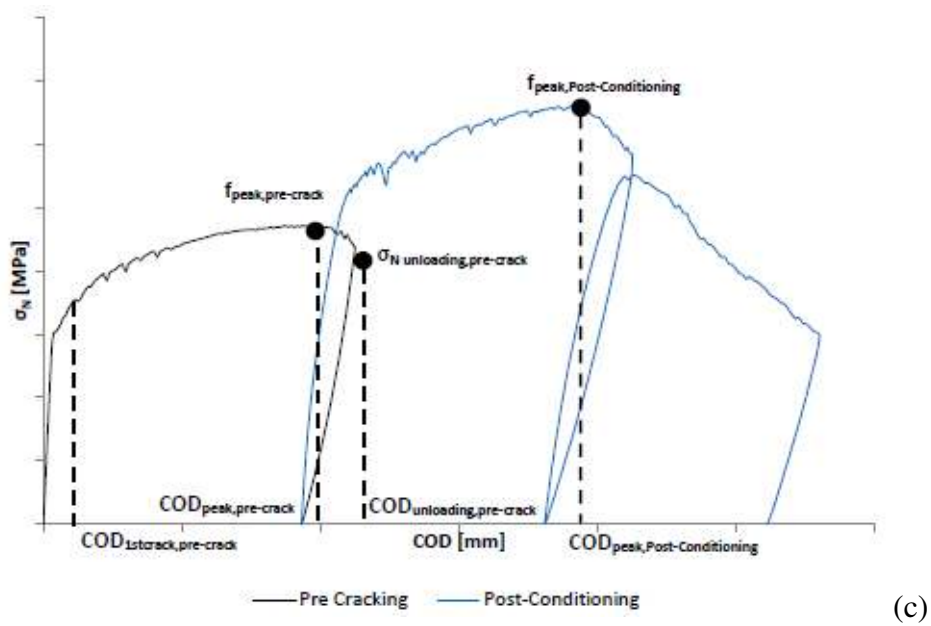
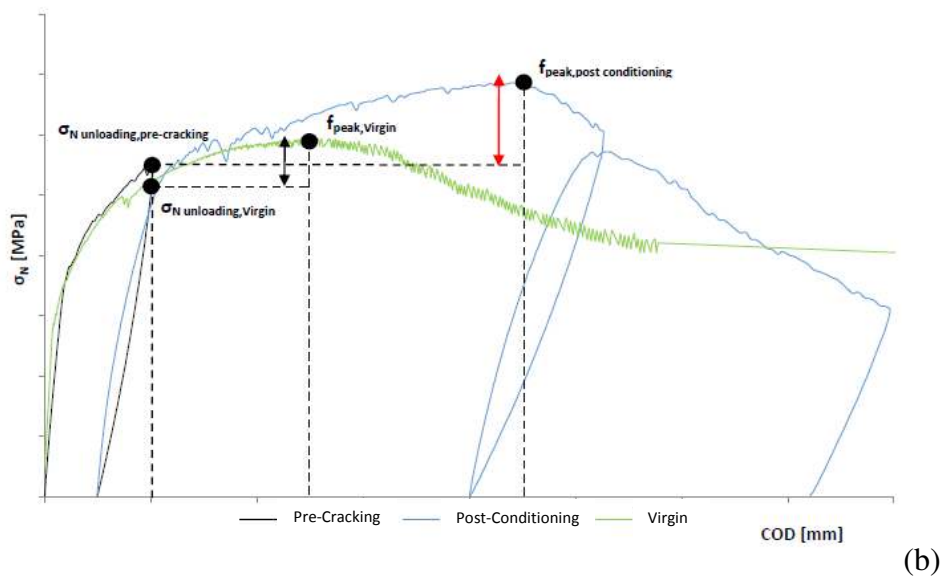
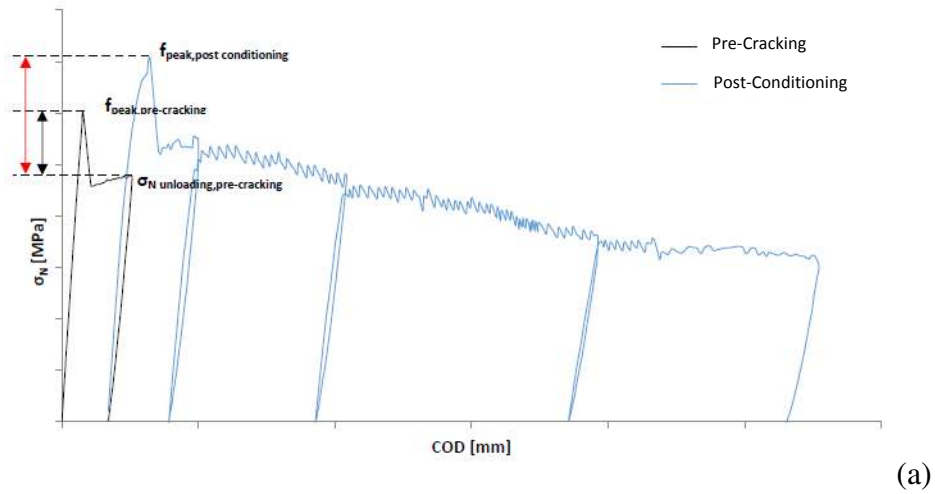


(b)

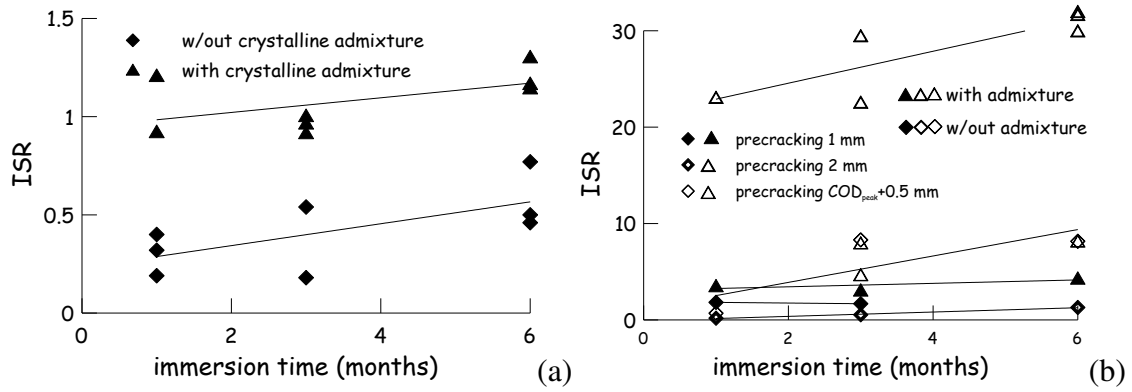


(c)

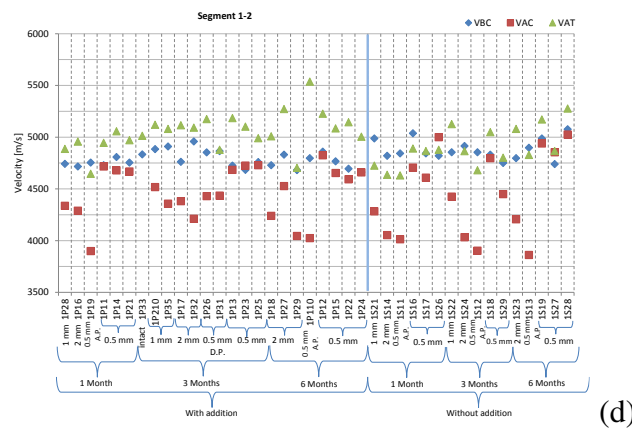
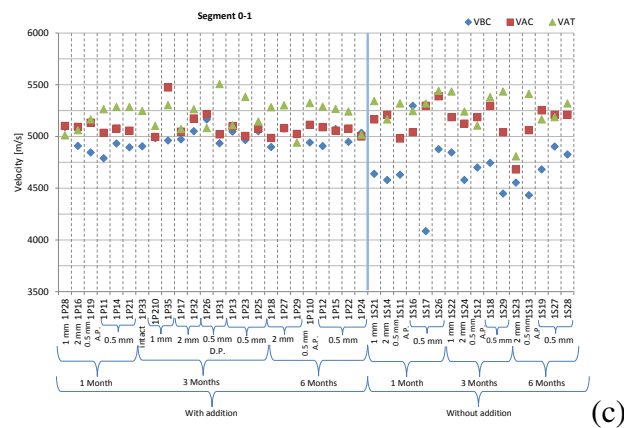
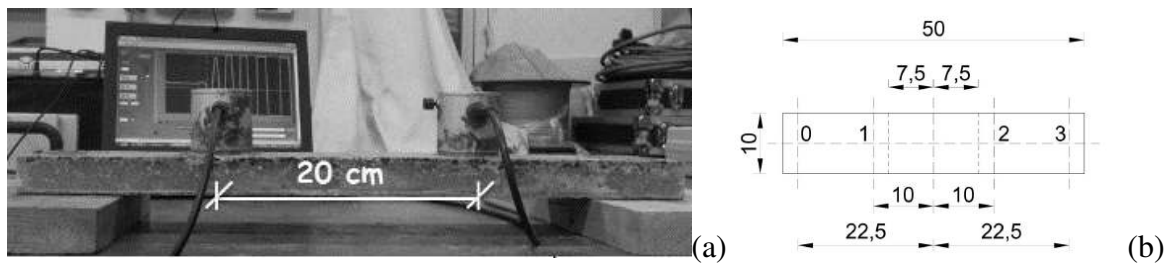
**Figure 12:** dimensionless  $\sigma_N$ -COD curves for deflection hardening specimens without and with the crystalline admixture, pre-cracked at 1 mm (a) 2 mm (b) and 0.5 mm after the peak (c) for different immersion times.



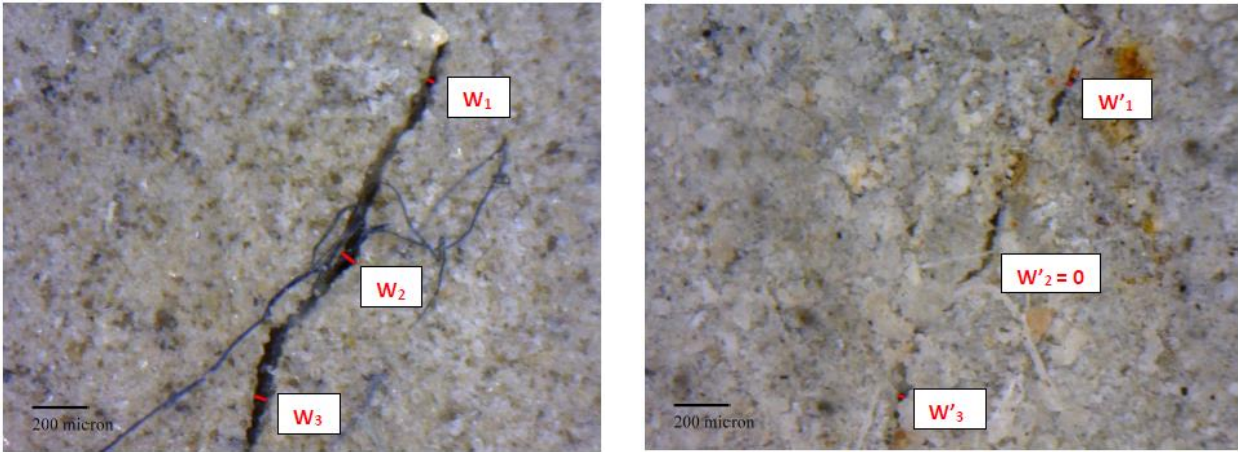
**Figure 13.** Definition of parameters to calculate the Index of Strength Recovery for deflection-softening (a) and hardening specimens pre-cracked in pre-peak (a) and post-peak regime (b).



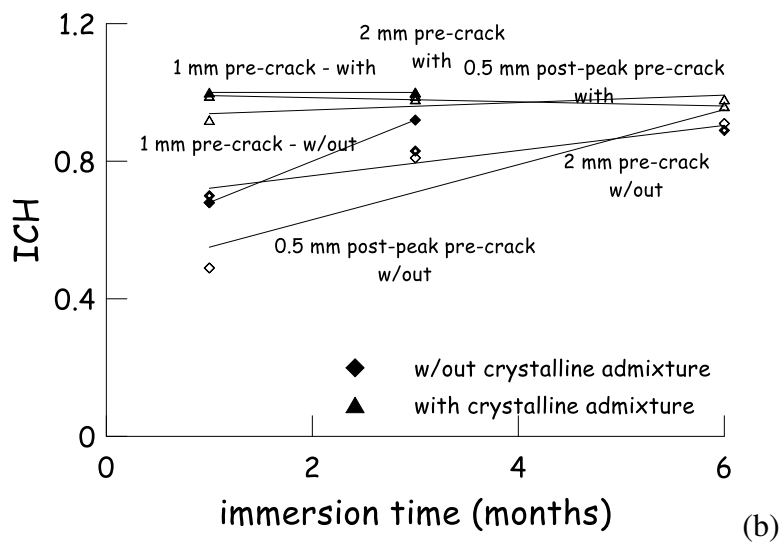
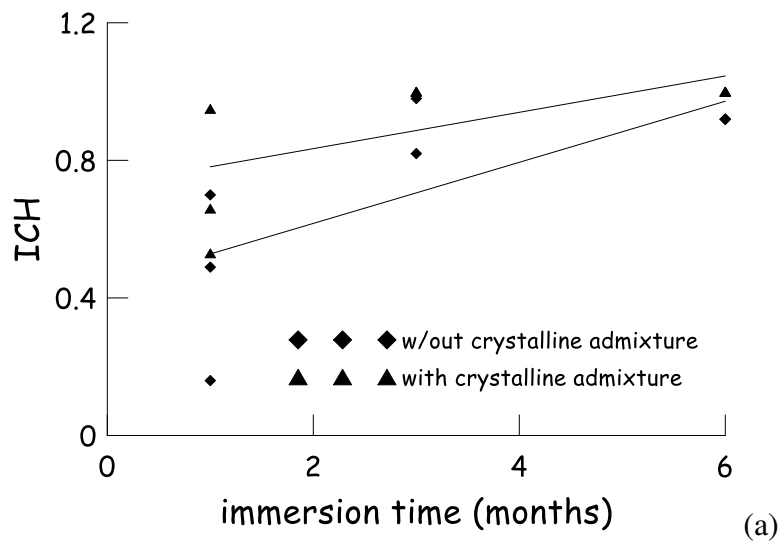
**Figure 14:** Index of Strength Recovery for deflection softening (a) and hardening specimens (b).




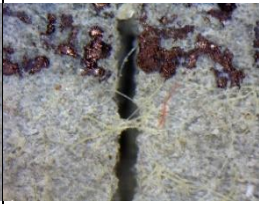

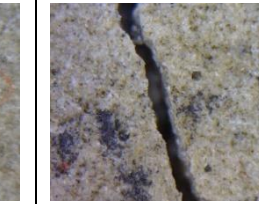

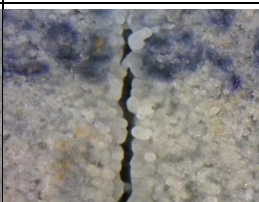


**Figure 15.** Set-up for UPV tests (a,b); UPV in the edge-uncracked (c) and central cracked (d) part of the specimens ( $V_{BC}$  = before cracking;  $V_{AC}$  = after cracking;  $V_{AT}$  = after conditioning treatment).





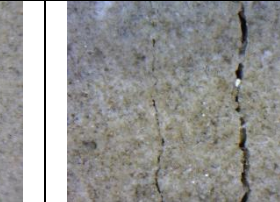

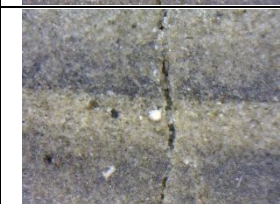
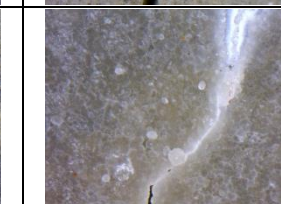

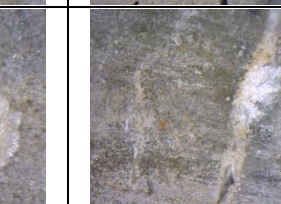
**Figure 16:** measure points for calculation of average crack width before (left) and after conditioning (right).



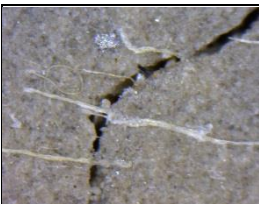
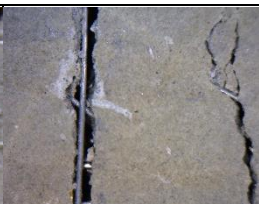

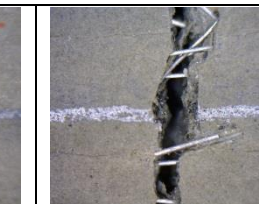




**Figure 17:** Index of Crack Healing for deflection softening (a) and hardening specimens (b).

			
			
1 month w/out addition ISR 0.41 IDaR 0.07 ICH 0.49	1 month with addition ISR IDaR ICH 0.66 <b>1P21</b>	6 months w/out addition ISR 0.77 IDaR 0.78 IAW 0.92	6 months with addition ISR IDaR ICH 1 <b>1P24</b>

(a – deflection softening specimens)

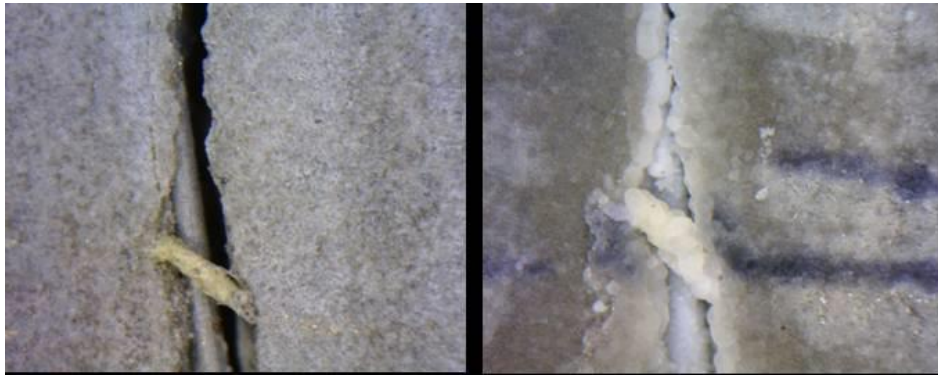
			
			
1 month w/out addition ISR 0.79 IDuR 0.07 IDaR 0.42 IAW 0.7	1 month with addition ISR IDuR IDaR IAW 0.99 <b>1P16</b>	6 months w/out addition ISR 12.58 IDuR 0.48 IDaR 0.63 ICH 0.89	6 months with addition ISR IDuR IDaR ICH 1 <b>1P29</b>

(b – deflection hardening specimens pre-cracked at 2 mm)

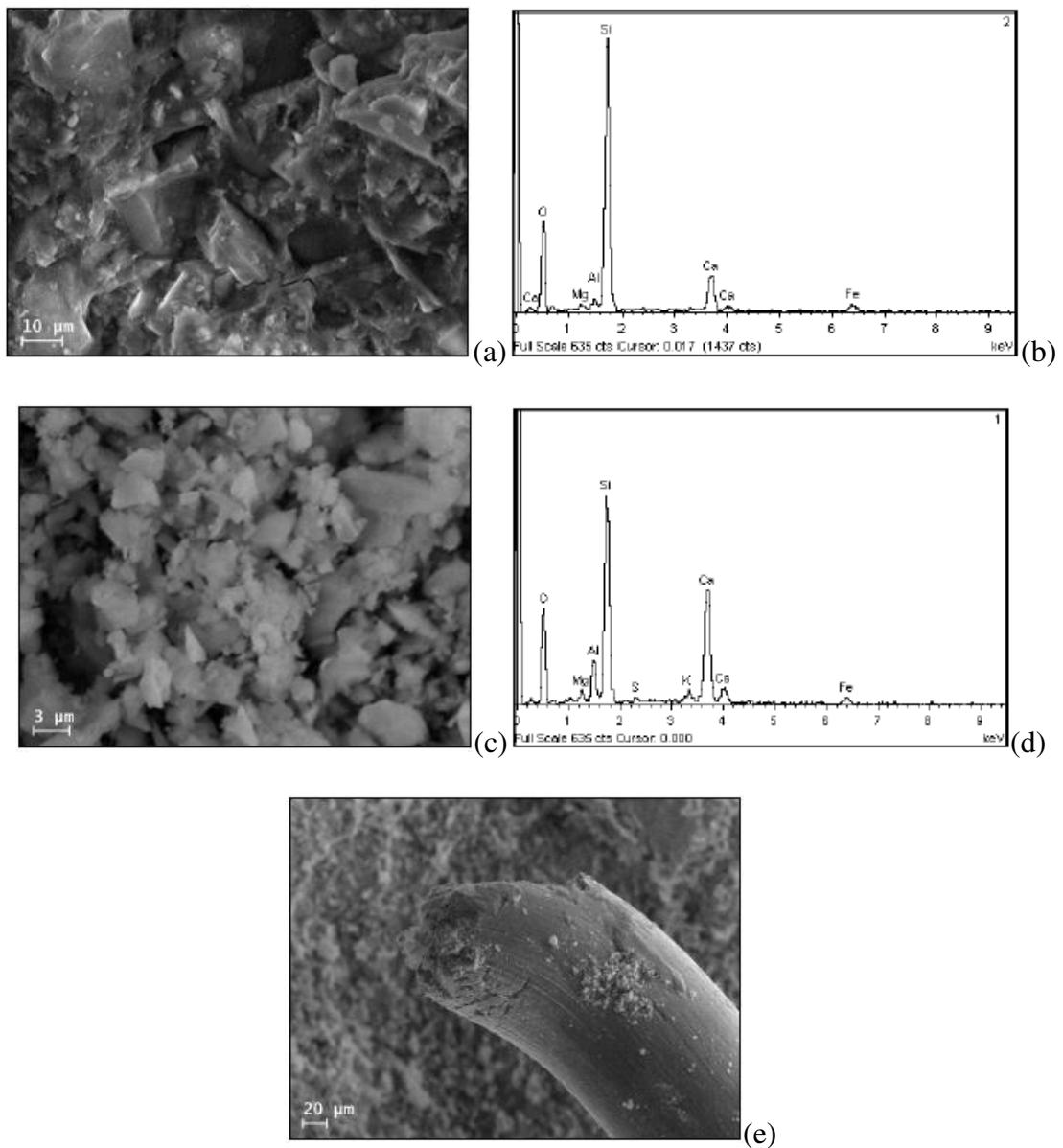
			
			
1 month w/out addition ISR 0.7 IDuR -0.8 IDaR 0.39 ICH 0.49	1 month with addition ISR IDuR IDaR ICH 0.92 <b>1P19</b>	6 months w/out addition ISR 8.31 IDuR -0.72 IDaR 0.72 ICH 0.91	6 months with addition ISR IDuR IDaR ICH 0.95 <b>1P110</b>

(c – deflection hardening specimens pre-cracked 0.5 mm after the peak)

**Figure 18.** Examples of healed cracks with related values of healing indices.



**Figure 19:** healing products deposited on fibres crossing the healing cracks.



**Figure 20:** microscope image (a,c) and chemical composition (b,d) of healed fractured surfaces of specimens without (a,b) and with (c,d) the crystalline admixture; healing products deposited on a fiber in the case of specimens containing crystalline admixture (e).